Haptic Handshank – A Handheld Multimodal Haptic Feedback Controller for Virtual Reality

K M Arafat Aziz[1] Hu Luo[1] Lehiany Asma[1] Weiliang Xu[2] Yuru Zhang[1,3] Dangxiao Wang[1,3,4]

[1]State Key Laboratory of Virtual Reality Technology and Systems, Beihang University, Beijing 100191, China
[2]Department of Mechanical Engineering, University of Auckland, Auckland 1142, New Zealand
[3]Beijing Advanced Innovation Center for Biomedical Engineering, Beihang University, Beijing 100191, China
[4]Peng Cheng Laboratory, Shenzhen 518055, China

ABSTRACT

Compared to wearable devices, handheld haptic devices are promising for large scale virtual reality applications because of their portability and capability of supporting large workspace haptic interaction. However, it remains a challenge to render multimodal haptic stimuli in handheld devices due to space confinement. In this paper, we present a modular approach to build a Multimodal Handheld Haptic Controller called "Haptic Handshank" that includes a thumb feedback component, a palm feedback component, and a motion tracking component. In the thumb feedback component, a compact pneumatically-driven silicone airbag is utilized to simulate softness, and a flexible membrane based on the electro-vibration principle which covers the top portion of the airbag for rendering virtual textures. In the palm feedback component, vibrational motors and Peltier devices are embedded into the device's body for rendering vibrotactile flow and distributing thermal stimuli. In the motion tracking component, an HTC-Vive tracker is mounted on the bottom of the controller's handle to enable 6-DOF palm motion tracking. The performance of the handheld device is evaluated through quantitative experimental studies, which validate the ability of the device to simulate multimodal haptic sensations in accordance with diverse hand manipulation gestures such as enclosure, static contact, rubbing, squeezing and shaking of a cup of cold drink in 3D virtual space.

Keywords: Multimodal, handheld device, haptic feedback, controller, virtual reality.

1 INTRODUCTION

Handheld haptic devices are promising for virtual reality applications because of their portability and capability of supporting large workspace for haptic interactions [1]. With recent advances in commercial head-mounted displays such as Oculus, MS HoloLens and Google Magic Leap, virtual reality (VR) is becoming a global mainstream phenomenon.

In today's VR systems, the advanced audio and visual content coupled with accurate motion tracking may fuel our desire more than ever to "touch and feel what we can see". However, due to the lack of compact haptic technology that can simulate realism at an affordable price, haptic feedback from handheld controllers available in the market today is limited to only vibrational flow. Although commercial handheld haptic devices exhibit many advantages in VR application, such as small form factor, lightweight, low cost, low power usage, and long usability, they are incapable of rendering multi-properties of simulated objects.

On the contrary, stimuli in real life are multimodal in nature conveying information such as impact forces, vibration, heat, texture, and so on [2]. High-fidelity simulation of real-time haptic sensations such as reaction forces, vibrations, textures, and temperature feedback from virtual objects to the user can create a sense of immersion in the virtual world.

The lack of user immersivity in VR scenario thereof necessitates novel handheld haptic devices that can render compound haptic stimuli to the users.

Presumably, sensory illusions such as shape, size, weight, texture, softness, and temperature are some of the crucial haptic cues that discern the properties of the object grasped in VR [3]. However, the spatial confinement of handheld controllers can undermine their ability to accommodate various hardware necessary for actuating the multi-properties. Thus, a combination of miniature actuation methods and novel collocation algorithm must be implemented to overcome the space restraint.

In this paper, we design a handheld haptic controller and integrate it with a pre-existing HTC Vive tracking module. We then propose a solution for simultaneously rendering the three fundamental haptic modalities (softness, texture and temperature) to the user's palm and fingers during interaction with virtual objects.

The contributions of this paper are in threefold:

1. By categorizing the five fingers' functions into two groups, we present a modular approach to render high-fidelity multimodal haptic stimuli within the compact space of a handheld controller. The thumb feedback component provides softness and texture feedback for supporting fine exploration of the thumb to slide along the surface of virtual objects. The palm feedback component provides vibrotactile flow and thermal stimuli for the other supporting four fingers and the palm.

2. To provide spatially collocated stimuli of softness and texture display to the users' thumb, a sandwich structure with soft actuating materials is proposed, in which a compact pneumatically-driven silicone airbag is utilized to simulate softness, and a flexible membrane based on the electro-vibration principle is overlaid on the surface of the silicone airbag to render virtual textures for the thumb.

3. Quantitative experimental studies are carried out to measure the performance of the device to simulate independent modality, along with the ability to simulate multimodal haptic sensations in accordance with diverse hand manipulation gestures such as

kmarafataziz@buaa.edu.cn hapticwang@buaa.edu.cn
yuru@buaa.edu.cn p.xu@auckland.ac.nz
cosmoluohu@outlook.com lehianyasma@buaa.edu.cn

978-1-7281-8508-8/20/$31.00 ©2020 IEEE
DOI 10.1109/ISMAR50242.2020.00047

enclosure, static contact, rubbing, squeezing and shaking of a cup filled with a cold drink in 3D space.

2 Related Work

Simulation of diverse haptic sensations is a requisite for reproducing multi-properties of virtual objects with satisfactory realism. Some properties of objects that add realism in the simulated environment are softness, texture, vibrotactile and thermal feedback to the user's hands and body.

2.1 Softness Feedback

Wearable haptic belt has been proposed for rendering softness of objects. Fani *et al.* [4] designed a wearable fabric-based display that uses motors to modulate the stretching state of elastic fabrics for achieving variable stiffness. The device can be implemented actively or passively for softness exploration using the index finger.

Pneumatic actuators have been explored for stiffness perception of virtual objects at both kinesthetic and cutaneous levels. Pneumatic-driven soft actuator with fiber-reinforcement [5] has been utilized by Zhang *et. al* [6] for achieving a two-finger soft force feedback glove. Using a pneumatic actuator, Sclingo *et al.* [7] demonstrated how normal indentation of contact area integrated with kinesthetic feedback can enhance softness perception.

There have also been attempts in combining pneumatics with jamming techniques for rendering stiffness and shapes of objects. Stanley *et al.* [8] implemented particle jamming combined with pneumatics to model a controllable cutaneous tactile display to feel softness and shape simultaneously.

Deformation of springs can also be used to achieve a variable softness display. Mansour *et al.* [9] designed a multimodal tactile display device that can emulate both the shape and stiffness of an object using an array of actuator pins made from shape memory alloy (SMA) springs.

2.2 Vibration and Texture Rendering

Mechanical vibrations from motors, LRA, or voice coil actuators can not only provide users with binary information but can also be modeled to enhance the experience associated with feeling textures of virtual surfaces during dragging action [10] and hardness of virtual surfaces during tapping action [11]. Some researchers have focused on capturing the vibrational flows produced from interactions with real objects and formulated a data-driven model that can be played back to the user [12].

Kuchenbecker *et al.* [13] developed a hand-mediated tool that captures the feel of real surfaces by sensing the forces, motion, and vibration associated with hand movement when interacting with physical objects and play it back remotely through an active stylus mounted with voice coil actuator.

Simulating surface textures to bare fingers via tactile displays fall under two main categories. The first one, known as squeeze film effect, generates mechanical vibration at ultrasonic frequencies on touch surfaces, where the frequency is modulated by piezoelectric actuators [14]. The second technology works on the electro-vibration principle, where thin insulated and conducting materials form paper-like layers and an alternating current is applied between the layers to generate the tactile effect on the surface to excite a sliding finger [15] or a thin slider [16].

2.3 Thermal Sensation

Design requirements of a thermal feedback interface for simulating heat transfer between the fingertip and the surface of a virtual object have been previously proposed in the literature [17]. Typically, an active thermal element such as the Peltier module along with a heat sensor and the temperature control loop is integrated to monitor the surface temperature of the thermal display.

There have been attempts at rendering thermal sensations to the face [18] and whole body via haptic suit [19] for eliciting realistic virtual climates. However, most wearable tactile haptic devices rather focus on presenting thermal cues to the fingertips [20][21], where thermal acuity is high and exposure of the area during object manipulation and material discrimination is unavoidable.

An alternative to Peltier devices has also been explored for thermal sensation for both hands and body. Günther *et al.* [22] simulated thermal feedback to the skin through the exchange of flowing liquids that pass through a network conductive tubes at different temperatures. Haptx gloves excel at simulating thermal sensation to the hand by injecting small amounts of microfluid [23].

However, the design of multimodal handheld haptic devices for VR application with an augmented thermal display that can achieve fast-response heating and cooling sensation within limited space has not yet been resolved [1].

2.4 Handheld Haptic Feedback Controllers

Considering the drawbacks of wearable and desktop devices, researchers have explored the use of handheld devices for haptic rendering. Choi *et al.* [24] developed the CLAW, which is a multi-purpose handheld controller that augments a typical VR controller with force feedback and actuated movement to the index finger. The device uses a servo motor coupled with a force sensor to actively render stiffness of virtual objects. A voice coil actuator enabled with position tracking allows users to synchronously feel textures of virtual surfaces using the index finger.

Whitmire *et al.* [25] introduced the Haptic Revolver: a handheld controller that renders fingertip haptics when interacting with virtual surfaces. Haptic Revolver's core element is an actuated wheel that raises and lowers underneath the finger to render contact with a virtual surface. As the user's finger moves along the surface of an object, the controller spins the wheel to render shear forces and motion under the fingertip.

Benko *et al*. [26] demonstrated NormalTouch and TextureTouch, which are two mechanically-actuated handheld controllers that render the shape of virtual objects through physical shape displacement, enabling users to feel 3D surfaces, textures, and forces that match the visual rendering.

Murray *et al.* [27] developed a variable shape and stiffness controller for virtual interaction. The tubular-shaped controller with an internal cavity for pressurized air is driven by a pneumatic control valve connected to an external pump. The controller body is made of elastomer resin fabricated with Bravias lattice geometries for material enrichment.

Zenner *et al.* [28] developed Shifty: a controller with physical proxy to solve the perception of the mass of heavy and light objects, as each object feels the same with respect to its inertia in VR. Without exerting noticeable active forces, Shifty can slowly and automatically change its kinesthetic feedback during runtime by shifting a weight along its main axis to change its rotational Inertia.

Researchers in Tactical Haptics designed a controller called Reactive Grip [29] which is capable of simulating frictional forces. When an object is grasped with this controller, the sliding contactor plates present under the palm induce in-hand shear forces and skin stretch that mimic the friction and shear forces experienced when holding the handle of a device, tool, or other equipment.

In summary, many handheld devices have been developed to provide multimodal haptic feedback to the user's palm or fingers. However, none of the devices has enabled users to feel the material properties such as softness, texture and temperature of the grasped object simultaneously. The underlying limitation arises either from the technical barriers in spatially collocating the hardware for achieving concurrent simulation of multiple modalities or that the device itself can become too cumbersome to be suitable for handheld applications.

3 Design Concept Of A Multimodal Handheld Device

3.1 Modular Concept and Design Requirements

When designing a multimodal haptic feedback device, it is a prerequisite to select which types of the stimuli should be simulated by the device. An object coming in contact with the human hand can send multiple sensory cues to the human brain corresponding to the object's physical properties. These haptic cues can be perceived through kinesthetic and proprioceptive channels of our bodies and they can provide important information that helps us in object perception and object recognition.

For instance, the reaction forces acting normal to the fingertip during grasping can determine the softness of the object, lateral forces from rubbing gestures determine the smoothness or texture of the object and thermal cues on the palm and fingers discern the thermal characteristic of the object so as to determine whether the object is perceived as hot, cool or moist by nature.

Previous studies have emphasized such three fundamental modalities of human haptic perception such as softness, texture, and temperature among other haptic cues [1][2][3]. There have been many attempts to combine two or more haptic modalities, but due to the bulky size of actuators, the resultant device has been a compromise with portability and usability for VR applications.

Hence, there is a strong need for compact lightweight haptic devices that are ergonomic in size and shape and allows free movement in space while eliciting high-fidelity haptic sensations to the user's palm and fingers. Thus, in order to mimic realistic touch sensations of virtual objects, the design goal of our haptic controller is to allow users to perceive three fundamental haptic modalities: softness, temperature, texture. In addition, vibrotactile feedback technology is well developed and vibrotactile stimuli can provide useful guidance or meaningful information to users. Therefore, we also integrate miniature vibrotactile actuators in our handheld device. Based on these ideas, we have established a set of design requirements for a useful multimodal haptic feedback controller for VR stated in Table 1

TABLE I
DESIGN REQUIREMENTS OF A MULTIMODAL HAPTIC CONTROLLER FOR VR

	Maintaining the functionalities of existing VR	Providing multimodal haptic feedback
1	Handheld for ease of use.	Ability to render the temperature of virtual objects.
2	6DOF supported by motion tracking in 3D space.	Ability to render forces from touching or grasping virtual objects such as elastic, inelastic stiffness, and shear force.
3	Ergonomically comfortable.	Ability to render textures of virtual surfaces.
4	Ungrounded device.	Render haptic effect for vibration resulting from shaking.

To meet the above requirements, one important design rationale of our device is based on the functional categorization of users' five fingers when we interact with the external world through a handle-grasping posture. It has been observed that in handheld applications, usually four fingers are used to hold and stabilize the handle, while the thumb is used for fine exploration, such as touching the surface of the object and to distinguish its texture and softness. The index finger can be moved from time to time in order to access trigger buttons. Based on the above two observations, as shown in Figure 1, we proposed a modular design of the multimodal hand-held device for virtual reality applications.

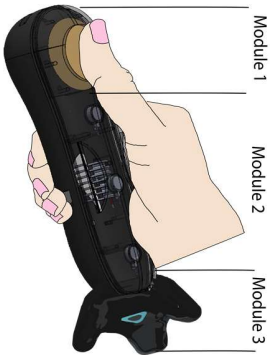

Figure 1: Modular design concept of a handheld controller for VR.

Module 1 represents the top part of the controller; Module 2 represents the handle body grasped by the palm and four fingers while Module 3 houses a tracking unit at the bottom of the device. Module 1 serves as the thumb feedback component, responsible for rendering softness and texture feedback to the user's thumb. Module 2 is the palm feedback component that can reproduce vibrotactile feedback and temperature display to the palm and to the remaining fingers. Module 3 constitutes a 6-DoF HTC Vive motion tracking component which is the motion sensor of our haptic controller. Detailed working principles and functionalities of each module are introduced next.

3.2 Design of the three components

3.2.1 Thumb feedback component

As shown in Figure 2, the thumb feedback component consists of a flexible thin membrane for texture display and a silicone airbag for softness feedback. The membrane is mounted on the top surface of the airbag, re-creating a combination of texture and softness. When the thumb pushes on the airbag and slides along the membrane, the pressing action of the thumb corresponds to softness feedback while the sliding action of the thumb corresponds to texture feedback.

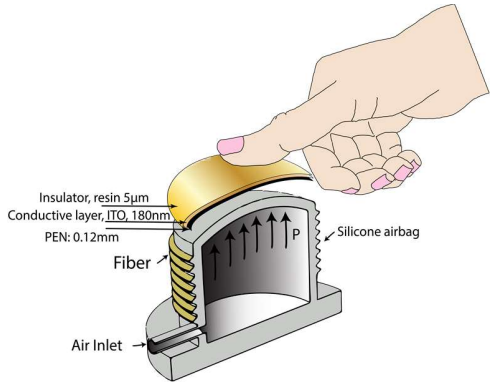

Figure 2: The layout of the thumb feedback component.

The thin texture membrane is adapted from the work of Guo *et al*. [30], which focuses on a flexible tactile interface, called FlexTouch. Based on the electro-vibration principle, the membrane is able to render different frictional forces by alternating the exciting voltage signals. A wide spectrum of frequency and amplitude of electro-vibration generated by the texture membrane creates an illusion of rubbing fingers on various surfaces when combined with visual feedback.

Underneath the texture membrane, there lies a soft cylindrical silicone airbag actuator with an internal cavity of 35mm. With the

fiber reinforcement around the circumference of the airbag's cylinder [5], the radial deformation of the airbag is constrained. When air is injected through the inlet, the airbag can only produce elongation along its axial direction. By controlling the air pressure inflated into the airbag, variable softness can be achieved.

With the sandwiched layout of the flexible thin membrane and the silicone airbag, the thumb feedback component is not only capable of providing a collocated texture and stiffness feedback but also ensures that only a small volume is occupied within the compact space of the handheld device.

3.2.2 Palm haptic feedback component

The palm feedback component, as shown in Figure 3, consists of three miniaturized vibrational motors and two Peltiers (with heatsinks) used for simulating vibrotactile and thermal feedback.

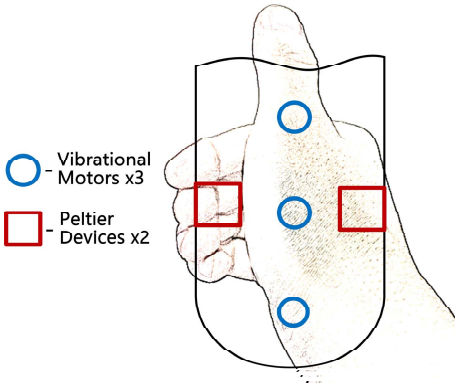

Figure 3: Palm component of the haptic Handshank showing the three vibrational motors and the two Peltiers that are embedded.

In order to produce diverse thermal feedback to the user, Peltier devices are mounted on key locations of the controller body. The layout aims to produce direct thermal sensation to fingers (except thumb), and on the thenar eminence at base of the thumb, which is reported to be the most thermally sensitive region on the glabrous surface of the hand [31]. Direct contact with the skin allows the Peltiers to convey a non-homogeneous temperature distribution of the virtual objects grasped by the user in a simulated environment

The three vibrational motors are mounted on the internal surface of the upper cap of the controller. The motors are placed with equal spacing to provide a distributed vibrotactile flow. A sequence of the vibrational motor turning on/off at different temporal resolutions is utilized to create an array of vibrational patterns.

3.2.3 6DoF motion tracking component

In the motion tracking component, an HTC Vive 6DoF tracker is used to track the movements of the controller in midair. The tracker is mounted at the bottom of the device using a ¼" screw. This integration enables the Haptic Handshank to spatially register the 6DoF movement of the handheld device with the virtual hand in the scene, thus allowing our controller to render diverse haptic stimuli in accordance with users' hand motion.

4 Design and Modeling of Each Haptic Modality

In order to render multimodal haptic feedback simultaneously, we first determine the actuation parameters and develop each modality separately. Then, we integrate the hardware and optimize the effect of each modality to achieve a real-time application of the combined system. With an ARM 32-bit microcontroller device embedded at its core, we create a real-time operating system (RTOS) application with our device and integrate it with an HTC headset and develop a demo in Unity 3D. In this section, the design and modeling process of each modality are presented in detail.

4.1 Softness Feedback

Humans generally assess softness by squeezing or indenting the objects within their finger pads [32]. The cutaneous information associated with the contact area pressure distribution helps us distinguish whether the object is stiff or compliant.

One observation is that during the handle gripping posture of hands, when asked to complete a single-finger pressing or sliding action, most people prefer their thumb finger. Another observation is that the surface area of the thumbpad is much larger than that of the index. Previous studies have shown that the contact area between the finger pad and the target object is important for the tactile perception of softness [33].

Considering the area of the thumbpad exposed to surfaces is larger than other fingers, much higher resolution of softness perception can be achieved with the thumb.

Due to space constraint prerequisites of handheld devices, we decide to place one pneumatically driven soft actuator of diameter 35mm under the thumbpad to maximize the area of exposure to skin and render softness display to the thumb. We adopt a pneumatically actuated soft silicone airbag to achieve distributed pressure on the thumbpad of the user. The softness display driven by air pressure includes three main parts: a silicone airbag, an air pump, and a proportional control valve comprising an in-built pressure sensor.

For manufacturing the airbag, we selected soft, stretchable material that imitates the characteristics of the skin, such as silicone rubber. For the convenience of fast production, we decide to use the liquid skin silicone rubber (Dragon Skin Series) from the American Smooth-On mold brand as the raw material. Its characteristics allow processing at room temperature, easy operation, and no shrinkage. Dragon Skin 10 is often used to imitate human skin and can achieve realistic biological effects. Also, it is relatively soft and suitable for simulating softness properties.

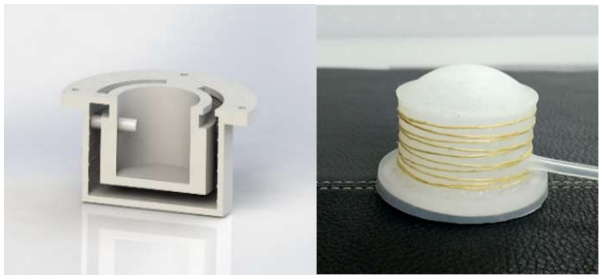

Figure 4: (Left) Mold for manufacturing the silicone airbag. (Right) Silicone airbag made from Dragon Skin 10 Series.

Combined with fiber reinforcement, the motion of elongation of the airbag is restricted to the vertical axis normal to the thumb. The airbag is connected to the pump through a 3mm diameter tube that runs along the controller and attaches to the pneumatic control valve. The proportional control valve being used is a controllable air pressure regulator with an automatic exhaust to the atmosphere.

Based on whether an object is grasped or not in the VR scene, the pressure inside the softness display can be controlled by outputting a reference voltage signal from the microcontroller to the proportional valve while the valve's closed-loop system with the in-built pressure sensor controls the amount of fluid entering the airbag.

The time needed for the airbag to inflate/ deflate as the signal fires are within 0-2 seconds. As long as the reference voltage signal is not changed, the air pressure within the chamber remains steady. With respect to the proportional valve's input reference signal range (0-5V), the output air pressure can be linearly varied between 1-900kPa (above room atmospheric pressure). The proportional control valve is externally powered by a DC voltage source of 24V/0.12A connected to the main supply.

The current device implements a passive pressure control; therefore, no external pressure sensors have been used under the thumbpad to actively detect the user's pressing force.

The stiffness generated by the airbag surface onto the finger can be modeled as a function of a single variable, that is, the air pressure. The stiffness is defined as:

$$k = \frac{dF}{dx} \tag{1.1}$$

where k is the stiffness, F is an approximate of the average load, and x is the average displacement of the airbag in the axial direction. The stiffness is also a function of surface curvature and can be represented as a function of internal pressure:

$$k = f(\rho, p) \tag{1.2}$$

where ρ is the surface curvature of the airbag chamber and p is the internal air pressure of the airbag chamber.

4.2 Texture Feedback

Most of the tactile devices in the past relied on mechanical vibration to present tactile sensations [34], however, the interest in generating tactile sensations on the thin flexible surface has increased recently as electro-vibration principle works with low power consumption and can generate a high dynamic range. Therefore, focusing on the improvement of texture perception of virtual objects using the Haptic Handshank, we adapt a thin flexible membrane from the previous work of Guo *et al.* [30], FlexTouch.

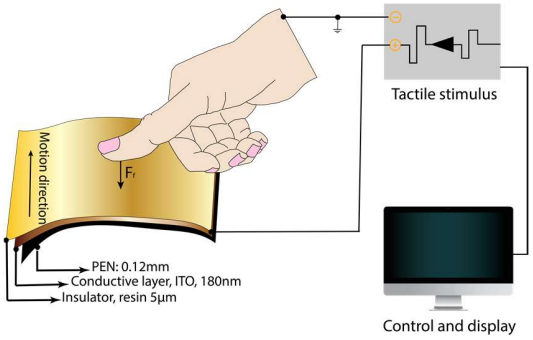

Figure 5: Operating principle of the FlexTouch membrane.

The FlexTouch is composed of three layers of conductive and insulation material as shown in Figure 5. A conductive transparent Tin Oxide (ITO) layer is wrapped above a Polythene Napthalate (PEN), coated by an insulator resin material on top that comes in contact with the finger. The overall thickness of the three layers is roughly 0.13 mm. The electro-vibration of FlexTouch depends on the magnitude and frequency of the applied voltage. Therefore, different tactile sensations can be created by controlling the amplitude and frequency of the applied voltage.

FlexTouch interface's ability to render various textures was highly influenced by the comprehension of basic human factors such as absolute detection threshold and Just Noticeable Difference (JND) perceived by the human touch. The absolute detection threshold of voltages amplitude which changes with the frequency of vibration can determine the baseline of user sensitivity when interacting with the device. Finding out the most sensitive frequency perceived at the lowest voltage amplitude was crucial for the design and implementation of FlexTouch.

When the fingers slide on FlexTouch, the electro-vibration increases the dynamic friction between the finger and the surface, and the change in dynamic friction can then be perceived as a change in texture, given that the finger is constantly moving on the surface. Although the membrane is neither as flexible nor as stretchable as the silicone airbag, it is flexible enough not to hinder the stiffness feedback while remaining impervious to strain.

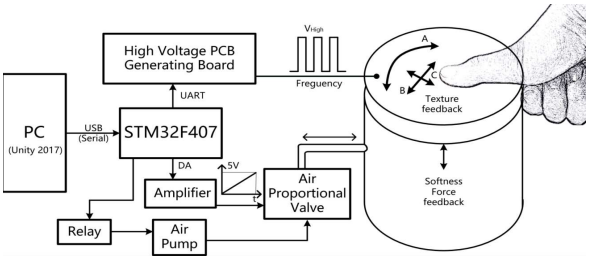

Figure 6: Control signal for the texture membrane and the softness feedback display.

When adding the texture layer on top, due to the inelasticity of the membrane and its restriction, the silicone airbag is constrained and renders the stiffness without elongating or changing shape. Whereas, when there is not much air inside, and due to the flexibility of the membrane, the thumb is capable of pushing downward and feeling the pliability of the silicone bag.

In summary, the thumb module comprises of the silicone airbag and a flexible thin membrane glued on top for providing a concurrent display of softness and texture, as shown in Figure 6. When an object is grasped in the virtual scene, the user's thumbpad will feel a distributed pressure from the softness feedback and as the thumb slides laterally along the surface, the user can feel electro-vibration from the texture membrane which corresponds to the texture of the object.

4.3 Temperature Feedback

Thermal displays that imitate the temperature of the material during hand-object interaction in simulated environments can undoubtedly enhance the user experience [17]. Our skin receptors sense the temperature of surrounding objects through differential temperature cues when contact is made. Thus, it is challenging to simulate thermal conditions for the brief moment of time at which the contacts with virtual objects occur, as to concurrently display the thermal properties of the contact material and trick the skin receptors with satisfactory realism [35].

For design consideration of thermal displays, it must be taken into consideration that certain parts of our skin possess a higher concentration of thermoreceptors than others, making them more sensitive to thermal cues. Studies have shown that, besides fingertips, the skin at the base of the thumb known as thenar eminence is remarkably sensitive to temperature changes and can resolve small changes in temperature thresholds [31][35], making the area a good candidate for mounting thermal display actuators.

Further design considerations of temperature display should take into account robust algorithms that can quickly change the surface temperature of the display and maintain the temperature with accurate sensing for augmenting realistic VR experience. Efficient cooling techniques must be explored to overcome heating of the overall device and maintain a homogeneous room-temperature inside the device so that the users can experience a change in temperature differential as soon as grabbing and dropping objects.

Here, our design challenge is to fabricate a miniature thermal actuation system to meet the compact space requirement of the handheld controller device. Also, the temperature feedback needs to have a fast response for a range of temperatures in order to quickly mimic the material properties of the virtual object grasped.

Ino *et al*. [36] constructed a Peltier-based thermal display to measure the change in finger temperature during contact as subjects tried to identify a range of materials such as aluminum, glass, rubber, polyacrylate, and wood. They found that the recognition rates for the various materials presented with the thermal display were equivalent to those measured using real materials with an accuracy of 66%.

Due to compact size and low power consideration, we adopted two small 10x10mm semiconductor Peltier devices as the heat source on either side of the controller, one placed near the area where the fingers rest and the other located at the base of the thumb.

A t-type thermocouple sensor integrated with the Max6675 chip is used to monitor the temperature of the Peltier. The sensor is mounted on the inner side of one of the Peltier to avoid error from contact with human skin.

Heatsinks are mounted on the other side of the TEGs to maintain a steady temperature differential to pump out the extra heat energy from the system. The overall effect increased the efficiency of temperature control by at least 35% and mitigates the chances of overheating the system during prolonged use.

A Proportional Integral (PI) controller was implemented to achieve the temperature control of the system with a fast response time. We derived the following control algorithm (shown in Figure 7) to drive the Peltiers for the temperature display.

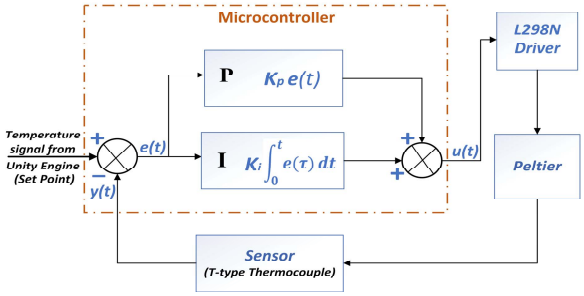

Figure 7: Temperature feedback loop and control algorithm for the Peltier devices.

An L298N full-bridge rectifier circuit is externally connected to a 12V DC source. The two Peltier modules form a series connection at the L298N output pins. Driven by a PWM signal from the microcontroller, the 12V/2A source was controlled by the PI algorithm, and polarity changed quickly to achieve high and low temperatures on one side. With heatsink added to the Peltiers, we can reach a temperature of 55°C from room temperature (ΔT ≈30°C) within 12-15 seconds.

4.4 Vibrational Feedback

Vibrotactile feedback has been the most primitive form of haptic feedback in devices for virtual reality applications due to two main reasons. Firstly, the integration of vibrational motors on haptic devices is straightforward and cheap. Secondly, because the human skin is well equipped to sense and interpret vibrations from their environment to gather information [2].

ERM vibrational devices are mature but the noise can be large and the delay is relatively high. On the other hand, LRA motors work on the basis of AC signals. Compared to ERM, although LRA can provide a richer tactile experience, lower power consumption solution and faster response time, however, they are expensive, they require additional drivers as well as a precise signal for achieving optimal vibration. Hence, for the sake of simplicity, we implement three brushed ERM motors.

Figure 8 shows the control signal from the microcontroller for both the ERM vibrational motors and Peltier devices implemented.

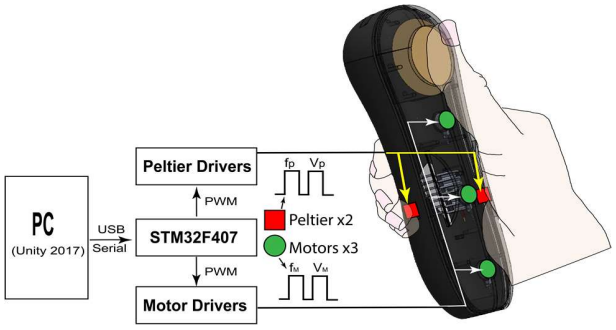

Figure 8: Control Signal for the vibrational and thermal feedback.

In order to achieve a practical data-driven vibration model, we implement 3 brushed miniature coin-sized DC vibrational motors (flat JL-1027, Shantou Jilai Co., Ltd, China) that offer the same form factor of LRA motors and can be easily controlled by a DC PWM signal from the microcontroller. Each motor is Φ10 mm in diameter with a nominal voltage of DC 3.0V and 70mA current. The nominal rotational velocity is 12000 ±2500 rpm. The three motors are evenly spaced with a 45 mm gap along a longitudinal line on the top housing of the controller.

Selective placement of vibrational motors can create diverse spatial-temporal vibrotactile patterns. With long term training, some of these patterns are easily recognized and thus can be encoded with meaningful haptic information such as directional cues used by Apple watch for navigation [37].

However, localizing DC eccentric rotating mass motors, to realize single point local vibration of multiple motors is difficult to attain. Even after implementing vibration isolation materials or vibration reduction mechanisms, such as damping, it is difficult to realize which particular motor is activated within such a narrow space inside the controller. Usually, the vibration of a single motor will cause the whole handle to vibrate. Thus, we place the motors farthest apart within the compact space of the hand-held device, 45 mm from each other to maximize the distance and increase the chances of perceiving localized vibration.

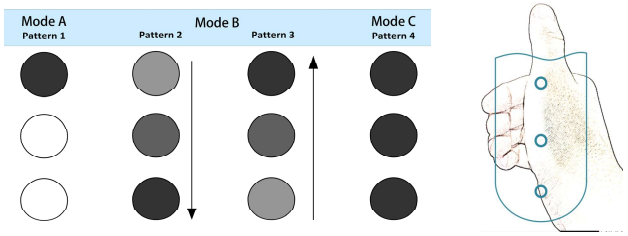

Figure 9: Vibration patterns generated by the vibrotactile display.

For the Haptic Handshank, we develop four distinct patterns of vibration using the three vibrational motors as shown in Figure 9. In Mode A, each motor is allowed to vibrate individually. Mode B allows two patterns of vibration. First, starting from the top motor and then one by one all the way to the bottom of the controller without time-lapse. Similarly, the second pattern of mode B allowing activation of motor one by one from bottom to top. Mode C allowed all 3 motors to vibrate at the same time.

These four candidate patterns were accompanied by five levels of vibration amplitude which were regulated by stepping up and down the exciting voltages (1V, 2V, 3V, 4V, 5V) through PWM signals from the microcontroller. The users can feel diverse vibrations based on interaction gestures and hand velocity in the VR scene. For example, when a person shakes their hand vigorously holding a Cola cup with ice in the VR scene, all 3 motors are activated. Otherwise, when hand movement with the cup is

slow, only one motor is activated. This way, much realistic haptic feedback can be conveyed to the users based on their interaction.

5 Mechatronic Design and Physical Prototype

5.1 Mechatronic Design

One of the core components of the Haptic Handshank is the single-chip STM32F407ZGT6: a 32bit microcontroller of ARM Core Embedded processor from STM electronics. A custom PCB based on this microcontroller is designed to communicate with the PC and produce control signals for all the actuators including the vibration motors, Peltiers, texture membrane, and the silicone airbag.

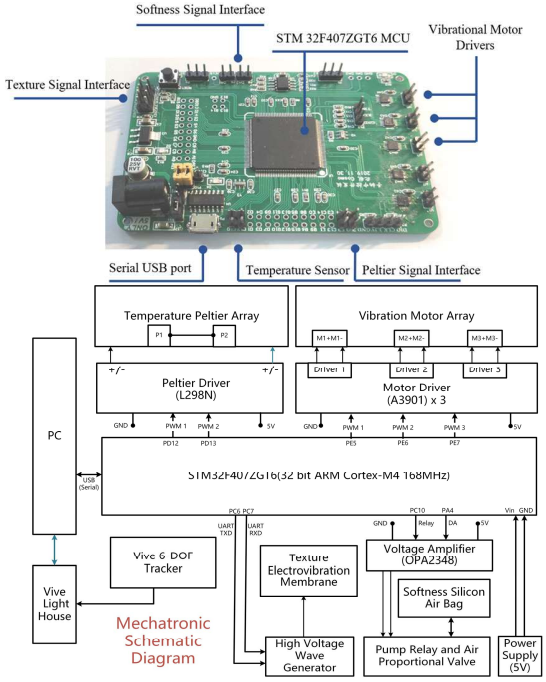

Figure 10: (Top) The PCB board developed for controlling the Haptic Handshank. (Bottom) Mechatronic system schematic of the Haptic Handshank.

The PCB showed in Figure 10 (top) is working as the central control board which is placed outside the controller body to create space for the actuator and the heat sinks. During the primary iterative phases of the device, the PCB board was initially embedded within the controller body. However, with added modalities, it became very challenging to effectively cool down the entire system without implementing additional hardware such as water cooler. However, the solutions for overcoming the heating challenge must not be bulky or cumbersome. Thus, we decide to make space for heat sinks and secure the PCB and connections outside in a control unit.

The power requirement for the central board at an idle state is measured at 5V/30mA and a maximum current of 600mA is needed to produce the signals for the actuators concurrently. Because vibration and temperature feedbacks are not continuously activated, we believe the power consumption of the current design is within the capability of an untethered battery-operated controller as long as the pneumatic unit is replaced with a mini portable pump.

The main PCB board communicates with the PC through the serial COM port. The Baud Rate is set at 192,000 bits/second. To produce the stimuli for texture, the MCU (STM32F407) receives UART commands from the virtual environment, and immediately a control command is sent to the High Voltage Wave Generator board (see figure 10 bottom) to produce high alternating voltage for activating the flexible membrane. Due to the round shape of the texture membrane, the thumb can only slide within the confined boundaries of the edges of the airbag.

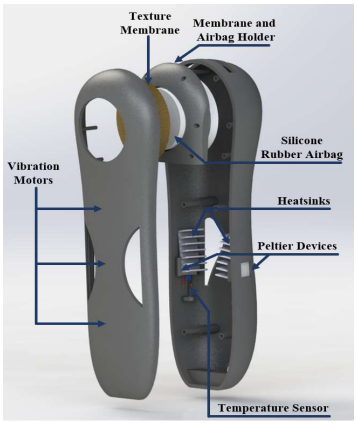

Figure 11: Detailed CAD model of the Haptic Handshank.

For simulating softness feedback, the DAC peripheral of the microcontroller sends a high-resolution controllable analog signal to the proportional control valve of the pump which results in quick inflation of the airbag cavity when an object is grasped or quick exhaust when the object is released (less than 2 seconds).

For simulating vibration, for example, when ice cubes inside a cup collide with each other, the motion of the hand is sensed as a function of time and a vibrational command with an exponentially decaying sinusoidal model is sent to the motors, resulting in a quick decaying response with respect to time.

For temperature feedback sensation, the upper controller sends commands to the microcontroller where a PI control algorithm is implemented. The t-type thermocouple senses the error and Peltiers are driven at a frequency of 1 kHz and 90% duty of PWM by the full-bridge driver to reach and maintain the target temperature.

The overall weight of the device integrated with the HTC Vive tracker is approximately 220 grams. Figure 11 shows the CAD model of the Haptic Hadshank.

5.2 A Virtual Cup Grasping Demo

Figure 12 shows the demo of grasping a takeaway paper Cola cup in Unity using the Haptic Handshank controller. Users can use the controller to pick up the cup from a table. When the Unity game engine detects a collision between the hand and the cup, the cup is grabbed onto the hand by sending commands to the microcontroller to initiate the pneumatic pump, the Peltiers and the texture membrane in order to activate the modalities.

Figure 12: Gestures and their corresponding haptic feedback in the VR scene. (a) grabbing and release objects (b) rubbing with the thumb to feel textures, (c) squeezing and pressing to feel the softness, (d) shaking to feel vibrations.

When the user performs a circular motion along the surface of the cup as shown in Figure 12- (b), he/she can feel the texture of the cup surface because of the modulated frictional forces produced by the flexible texture membrane.

When the user presses his/her thumb to squeeze the disposable cup as shown in Figure12-(c), he/she can feel the softness of the cup due to the outward contour of the airbag pressing against the finger. Most importantly, the user can move his/her thumb to perform a combined motion of squeezing and sliding, thereby he/she can perceive texture and softness of the cup simultaneously.

During the manipulation of the cup, the device can also simulate the cold sensation of the liquid mixed with ice. The Peltier devices are activated to maintain steady temperature via a PI feedback control loop. Similarly, if the user is grasping a hot cup of coffee in a VR scene, the Haptic Handshank can promptly simulate a quick response to change the temperature and maintain the temperature at a desired steady value for some time (10-13 seconds) to thermally support the interaction with the object.

When the user shakes the cup, commands are sent to activate all the vibrational the motor as a function of hand movement speed. Thus, the users can feel the vibrational sensation of ice cubes inside the cup colliding with each other upon vigorously shaking the cup. Finally, as the user releases the cup back towards the table, when a collision is detected between the cup and the table, the cup is dropped from the hand, and all the actuators are deactivated.

6 Experimental Evaluation

In this section, we discuss the experimental setup for evaluating the dynamic performances achieved with each modality.

6.1 Softness Feedback Experimental Setup

The goal of this experiment was to measure the range of stiffness that can be generated by the softness feedback module.

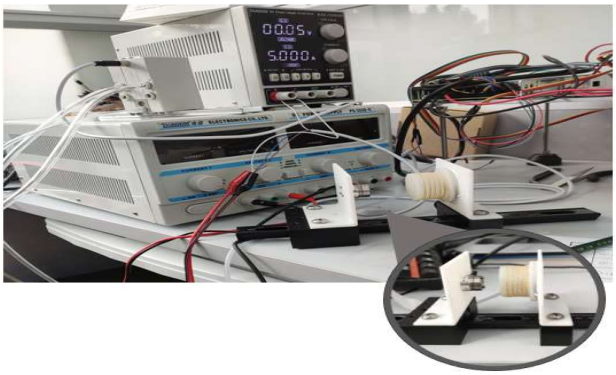

Figure 13: Experimental setup for testing the softness feedback.

An ATI Nano 17 Sensor (70N max) was used for collecting force reading from the silicone airbag at varying pressure. The force sensor and the airbag were fastened to two ends of a fixable scale. The airbag was attached to an SMC pneumatic proportional valve model ITV0050 which can output maximum air pressure of 0.9MPa. The pneumatic valve regulated a 3.0L capacity 1/6 HP pump externally connected to the main supply. Reference voltage signals were sent to the pneumatic valve controlled by a DC voltage source. Voltage signals from the DC source were manually regulated by a knob to control the output pressure from the pump.

The Force Sensor was connected to the computer through the Data Acquisition System (DAQ). Force readings from the airbag normal to the direction of expansion were shown on the Z-axis. The other two axes showed little or no reading. The output from Z-axis was exported to an Excel file. Three readings were taken at small distance intervals (x mm) away from the airbag at five constant pressure readings. The average of the three readings was calculated and used for the consistency of the data. The Force readings (in Newtons) were plotted against distances from the airbag (in mm.) as shown in Figure. 14.

6.1.1 Results & Discussion

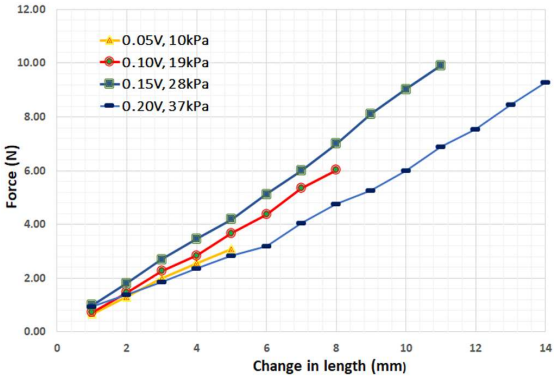

Figure 14: Stiffness profile of softness feedback at varying voltage signals sent to the pneumatic valve.

The curves at 0.05V, 0.10V and 0.15V show a linear relationship with the change in pressure. However, increasing the voltage signal above 0.15V, it is observed that the curvature of the line is inconsistent and the gradients of the line fall below that of 0.15V (as seen with 0.20V signal).

"Change in length" refers to the elongation of the airbag along the vertical axis. The gradient of each curve relates to the stiffness that can be perceived with respect to the reference input signal, as per equation (1.1). The rise of slope between 0-0.15V signals suggests variable stiffness within this range. However, the plummeting of gradient after 0.15V signal is observed because, after an increment of air pressure above 30kPa, the relationship between the change in length and input pressure is no longer elastic, resulting in a polynomial curve.

Hence, we use the pressure between the range of 0.05V to 0.15V to simulate objects of various stiffness. Within this range, the average stiffness that can be simulated by the airbag is determined to be between 0.6-0.89N/mm. The maximum stiffness achieved by the silicone airbag is found to be 0.9 N/mm. Based on the above observations, it can be concluded that the softness feedback device designed in this paper can achieve the rendering of fixed softness within its stiffness simulation range.

6.2 Temperature Feedback:

One important phenomenon of the Peltiers is called the Seebeck effect, which states that as long as there is a temperature differential between the plates, electricity can be generated. This technique can be integrated with the unexposed (to skin) side of the Peltier to introduce a small cooling effect, where thermoelectric cascading can convert the extra heat into energy and drive a load outside of the controller whenever the system overheats.

In order to explore the efficiency of cooling Peltier devices using thermoelectric cascading for handheld VR applications, here, we set up four experiments to test our temperature feedback system using Peltier devices driven by12V/2A DC power supply.

6.2.1 Experimental Setup:

A t-type thermocouple is used with integrated Max6675 IC for accurate temperature sensing. An L298N full-bridge rectifier circuit is used to drive the 10x10mm Peltiers using a 12V/2A DC adapter. An Arduino board is used to send a PWM signal to control the 12V/2A DC supply to the Peltier. An LTC3108 IC is used with

another Peltier to drive an external LED from the energy harvested (from waste heat). The second 10x10mm Peltier was cascaded below the driven Peltier as shown in the picture. A 10x35x10mm heat sink was used with and without Peltier cascading. Temperature rise and drop from the hot side of the Peltiers were analyzed with respect to time for four cases as shown in Figure 16. For each case, the experiment was repeated three times and the average values were calculated and used as the experimental results.

Case 1: No cooling techniques were used.

Case 2: A heatsink was added to the hot side.

Case 3: Peltier cascading with second Peltier added to the hot side for harvesting from waste heat.

Case 4: Peltier cascading with second Peltier scavenging waste heat along with heatsink.

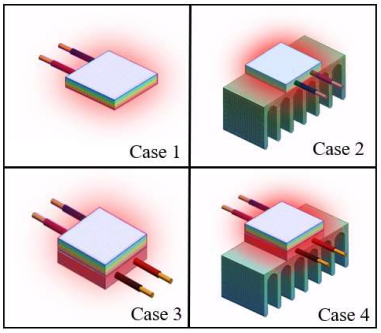

Figure 15: Experimental setup of four cooling techniques for Peltiers. The heat profiles illustrate the hot and cold sides represented by colors red and blue respectively.

6.2.2 Results & Discussion

The Peltiers were supplied with 12V/2A power for the first 60 seconds, then the power was cut off and the Peltier temperature was logged for an additional three minutes. It was observed that the maximum temperature from the Peltier device achieved without any cooling at 12V/2A was 93°C. The cold side temperature can go below 10 degrees, however, due to the ambient room temperature picked up by the sensor, the reading from the cold side can be inaccurate. Thus, we disregarded the cold side and regulated the hot side to derive data for cooling techniques.

It should be noted that the thermal display only serves as a constant temperature source, which maintains the interface temperature during contact. Its own thermal properties do not influence the heat transfer within the skin.

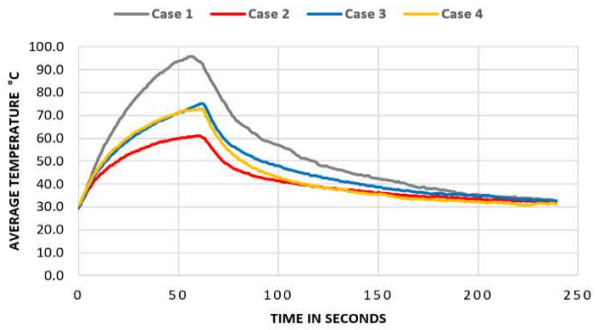

Figure 16: Curves showing the temperature comparison on the hot surface of Peltier implementing different cooling techniques.

In comparison between the data, the second case, where only a heat sink is added, showed the most significant cooling. It can be observed that the rise in temperature is slower than the other curves, the average maximum temperature achieved in the second case is about 60°C. Also, the heat dissipation rate is faster in Case 2 and Case 4 compared to Case 1 and Case 3.

Overall, cooling was boosted at least by 35% by adding heat sink, as higher heat exchange is achieved with the greater surface area. Therefore, it is recommended to add a heat sink to Peltiers for small compact devices in order to avoid overheating. Also, given the same layout, increasing the size of heatsinks can add surface area for cooling, thus a much bigger heat sink can expedite the cooling process further and avoid heat accumulation in one particular area.

Although energy harvesting from the heat source may seem an innovative approach to utilize the scavenging heat, unfortunately, it does not capacitate the need of rapid cooling. The thermal energy from the hot Peltier dissipates gradually as the surface area for heat transfer to the next Peltier is not large, which hinders the cooling effect.

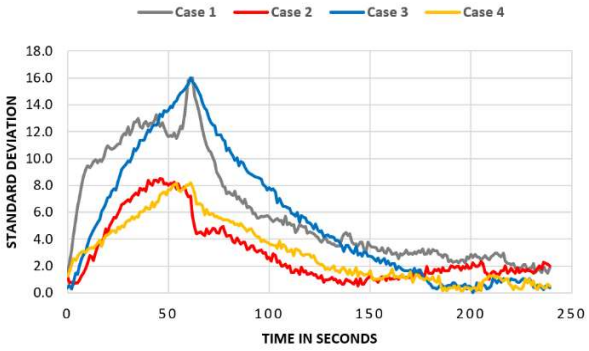

Figure 17: Curves showing the standard deviation between the readings obtained for each Case.

Figure 17 shows the Standard Deviation between the three data obtained for each case. The average Standard Deviation for each case is found to be as follows- Case 1: 6.04°C, Case 2: 2.98°C, Case 3: 5.49°C, Case 4: 3.03°C. The Standard Deviation values suggest that temperature gain and heat dissipation of the Peltiers is more uniform in Cases 2 and 4 with the added heatsinks and this phenomenon can be utilized to design a robust temperature feedback loop for thermal display because the reading picked up by the sensor are more reliable.

6.3 Vibrational Feedback

In order to understand human's perceptual performance of different vibrotactile patterns, a small study with 10 subjects was performed. The goal of the experiment was to measure their ability to recognize major vibrotactile flow patterns rendered on our handheld device.

6.3.1 Experimental Setup

Ten participants from Beihang University (7 males and 3 females) were recruited for 15 minutes of experimental sessions. The participants ranged from 22 to 28 years of age with an average age of 25. The participant sat in front of a computer screen and held the controller prototype in their right hand. All participants signed on a written consent form after they had been informed of the objective and procedure of the experiment. The experimental procedure was approved by the State Key Laboratory of Virtual Reality Technology and Systems of China and was in accordance with ethical standards.

The four candidate vibrotactile patterns were introduced and the participants were given examples of each pattern as preliminary training for five minutes. After the training period, the participants wore a pair of head-mounted earmuffs (Peltor H10A, 3M Inc.) for noise cancellation and an eye mask to block their vision. Four sets of questionnaires were presented with an increasing level of

difficulty. There was no time constraint for providing the response. The participants were asked to distinguish the patterns in the following order:

Task 1: Determine whether the vibration is local (Mode A) or upward/downward flow (Mode B)?

Task 2: Determine whether the vibration is local (Mode A) or global vibration (Mode C)?

Task 3: Determine whether the vibration is an upward flow or downward flow? (distinguish between Mode B)

Task 4: Determine whether the vibration is local, global, upward, or downward?

Figure 18: One participant is participating in the vibrotactile pattern experiment.

6.3.2 Results & Discussion

Task 1, Task 2, and Task 3 had six questions each and Task 4 had nine questions. The results of each Task were calculated as a percentage of the correct and wrong answers collectively from all the participants.

When asked to distinguish between only two patterns such as in Tasks 1, 2, and 3, it was observed that the participants answered confidently, which boosted their scores. However, Task 4 seemed to confuse participants as there were four patterns to choose the right answer from. Thus, the participants asked more time to confirm each pattern but for the sake of fairness, the patterns weren't repeated even though there have been requests on Task 4. The bar chart in Figure 19 shows the average performance and the standard deviation of the participants.

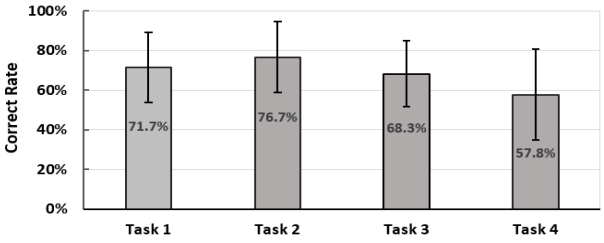

Figure 19: Results of vibrotactile perception experiment according to the average and standard deviation of correct rates.

From the experimental results, it is observed that participants performed better when asked to distinguish only between two vibrational patterns at a time. The standard deviation for Tasks 1, 2, and 3 ranged between 16-18% whereas the standard deviation for Task 4 was computed to be 24% with an average score of only 57.8% correct rates.

The result from our experiment suggests that using fewer motors and placing them farther apart in a handle can increase the identification rate of vibrotactile patterns for handheld applications, especially when subjects are asked to distinguish between local and global vibration flow.

Common vibrational actuators typically produce vibrations at frequencies above 100 Hz, which primarily activate the Pacinian corpuscles. The Pacinian corpuscles have large receptive fields [38], therefore, it is difficult for users to distinguish actuators when they are placed close together. As a consequence, the results in Tasks 1 and 2 reflect that the accuracy can be improved by placing the motors farthest apart.

However, in Task 4, the correct rate of determining only between local or global vibration dropped significantly to 55% from an average of 73% previously. This suggests that test subjects are susceptible to answer the same Tasks incorrectly when presented with too many choices without long term training sessions. Also, the amplitude of vibration can influence the perception of vibration. It was observed that the participants had difficulty identifying whether the pattern was a local or global vibration when the PWM signal from the microcontroller was below 3V.

It was observed that the identification of upward and downward flow among participants has been consistent in both Tasks 2 and 4, close to 70% accuracy. Hence, from these results, it can be derived that vibrotactile patterns can be designed to provide directional cues for the handheld haptic device.

7 Conclusions and Future Work

In this paper, we presented the modular design concept of a multimodal haptic controller, called Haptic Handshank, which augments a typical VR handheld controller with the simulation of softness and texture feedback to the thumb along with vibration flow and thermal feedback to the palm. The device is compact and capable of simulating haptic feedback in accordance with diverse hand gestures: touching, grabbing, pressing, rubbing, and shaking.

Experiments were carried out to quantify the fidelity and performance of each modality. Results from the experimental analysis suggest that a wide range of stimuli can be simulated for each modality within the compact space of a controller. The preliminary demo proves that the controller shows a promising feat in providing multimodal haptic feedback for handheld tasks where our controller responds quickly to change in the virtual environment and simulates high-fidelity sensations corresponding to the various handheld interaction gestures.

There are several limitations that need to be addressed in future work. Firstly, operating a 3.0L pneumatic pump and control valve is not a viable solution for home-usage. Miniature pneumatic actuation devices such as Mitsumi 6V/200maH DC rotary pump can be applied to make the entire system compact and portable.

Secondly, the texture sensation is produced by roughly modulating the frictional forces which are not being registered with the user's thumb movement. In order to produce fine textures, an additional motion-tracking sensor to measure the movement of the thumb is required. One possible solution is to mount a camera such as the LeapMotion sensor on the HMD, thereby tracking the thumb's motion.

Also, the heat sinks placed in cohesion with Peltier devices for enhancing the cooling effect might have ensured a simple design but at the cost of low heat transfer efficiency. Long periods of usage will cause internal heat accumulation resulting from Peltier devices thus overheating the entire system eventually.

Last but not least, the device remains tethered to the power source and for communication purposes with the PC. This issue can be resolved by introducing radio communication along with a DC source for powering the controller and a miniature pump.

We hope our work will spark more interest in research towards multimodal haptics and inspire novel handheld devices so that VR interactions become more natural and intuitive in the near future.

Acknowledgment

This work is supported by the National Key Research and Development Program under Grant No. 2017YFB1002803.

REFERENCES

[1] D. Wang, K. Ohnishi and W. Xu, "Multimodal Haptic Display for Virtual Reality: A Survey," in *IEEE Transactions on Industrial Electronics*, vol. 67, No. 01, pp. 610-623, Jan. 2020. doi: **https://doi.org/10.1109/TIE.2019.2920602**

[2] H. Culbertson, S. B. Schorr and A. M. Okamura, "Haptics: The present and future of artificial touch sensation," in *Annual Review of Control, Robotics, and Autonomous Systems 1*, pp. 385-409, 2018. doi: **10.1146/annurev-control-060117-105043**

[3] D. Wang, Y. Guo, S. Liu, Y. Zhang, W. Xu, J. Xiao, "Haptic display for virtual reality: progress and challenges," in *Virtual Reality & Intelligent Hardware,* vol. 1, no. 2, pp. 136-162, 2019. doi: **https://doi.org/10.3724/SP.J.2096-5796.2019.0008**

[4] S. Fani, S. Ciotti, E. Battaglia, A. Moscatelli and M. Bianchi, "W-FYD: A Wearable Fabric-Based Display for Haptic Multi-Cue Delivery and Tactile Augmented Reality," in *IEEE Transactions on Haptics*, vol. 11, no. 2, pp. 304-316, 1 April-June 2018, doi: **https://doi.org/10.1109/TOH.2017.2708717**

[5] P. Polygerinos, Z. Wang, B. Overvelde, K. Galloway, R. J. Wood, K. Bertoldi, *et al.*, "Modeling of soft fiber-reinforced bending actuators," in *IEEE Transactions on Robotics,* vol. 31, no. 3, pp. 778-789, 2015. doi: **https://doi.org/10.1109/TRO.2015.2428504**

[6] Y. Zhang, D. Wang, Z. Wang, Y. Wang, L. Wen and Y. Zhang, "A two-fingered force feedback glove using soft actuators," in *IEEE Haptics Symposium (HAPTICS), pp. 186-191, 2008*. doi: **https://doi.org/10.1109/HAPTICS.2018.8357174**

[7] E. P. Scilingo, M. Bianchi, G. Grioli and A. Bicchi, "Rendering Softness: Integration of Kinesthetic and Cutaneous Information in a Haptic Device," in *IEEE Transactions on Haptics*, vol. 3, no. 2, pp. 109-118, April-June 2010, doi: **https://doi.org/10.1109/TOH.2010.2**

[8] A. A. Stanley, J. C. Gwilliam and A. M. Okamura, "Haptic jamming: A deformable geometry, variable stiffness tactile display using pneumatics and particle jamming," in *2013 World Haptics Conference (WHC)*, Daejeon, pp. 25-30, 2013. doi: **https://doi.org/10.1109/WHC.2013.6548379**

[9] N.A. Mansour, A.M.R. Fath El-Bab and M. Abdellatif, "Design of a novel multi-modal tactile display device for biomedical applications," in *The Fourth IEEE RAS/EMBS International Conference on Biomedical Robotics and Biomechatronics*, pp. 183-188, 2012. doi: **https://doi.org/10.1109/BioRob.2012.6290860**

[10] S.J. Lederman, R.L. Klatzky, C.L. Hamilton and G.I. Ramsay, "Perceiving surface roughness via a rigid probe: Psychophysical effects of exploration speed and mode of touch," in *Haptics-e (Electronic Journal of Haptics Research),* vol. 1, no. 1, pp. 1-20, 1999.

[11] T. Hachisu, M. Sato, S. Fukushima and H. Kajimoto, "Augmentation of material property by modulating vibration resulting from tapping," in *International Conference on Human Haptic Sensing and Touch Enabled Computer Applications*, pp. 173-180, Springer, Berlin, 2012. doi: **https://doi.org/10.1007/978-3-642-31401-8_16**

[12] A. Y. Takeuchi, S. Kamuro, K. Minamizawa and S. Tachi, "Haptic duplicator," in *Proc. ACM Virtual Reality Int. Conf.*, pp. 30–31, 2012. doi: **https://doi.org/10.1145/2331714.2331749**

[13] K.J. Kuchenbecker, J.M. Romano and W. McMahan, "Haptography: Capturing and Recreating the Rich Feel of Real Surfaces," in *Robotics Research: the 14th Int'l Symp. (ISRR '09)*, vol. 70, pp. 245-260, 2011.

[14] P. Laitinen and J. Menp, "Enabling mobile haptic design: Piezoelectric actuator technology properties in handheld devices," in *IEEE International Workshop on Haptic Audio Visual Environments and their Applications (HAVE 2006)*, pp. 40-43, 2006. doi: **https://doi.org/10.1109/HAVE.2006.283787**

[15] O. Bau, I. Poupyrev, A. Israr, and C. Harrison, "TeslaTouch: electrovibration for touch surfaces," in *Proceedings of the 23rd annual ACM symposium on User interface software and technology*, New York, New York, USA, 2010. doi: **https://doi.org/10.1145/1866029.1866074**

[16] A. Yamamoto, S. Nagasawa, H. Yamamoto and T. Higuchi, "Electrostatic tactile display with thin film slider and its application to tactile telepresentation systems," in *IEEE Transactions on Visualization and Computer Graphics*, vol. 12, no. 2, pp. 168-177, March-April 2006. doi: **https://doi.org/10.1109/TVCG.2006.28**

[17] L. A. Jones and H. Ho, "Warm or Cool, Large or Small? The Challenge of Thermal Displays," in *IEEE Transactions on Haptics*, vol. 1, no. 1, pp. 53-70, Jan.-June 2008. doi: **https://doi.org/10.1109/TOH.2008.2**

[18] R. L. Peiris, W. Peng, Z. Chen, L. Chan, and K. Minamizawa. "ThermoVR: Exploring Integrated Thermal Haptic Feedback with Head Mounted Displays," in *Proceedings of the 2017 CHI Conference on Human Factors in Computing Systems (CHI '17).* Association for Computing Machinery, pp. 5452–5456, New York, NY, USA, 2017. doi: **https://doi.org/10.1145/3025453.3025824**

[19] Teslasuit: Full body haptic feedback platform for Virtual and Augmented Reality. https://teslasuit.io/blog/teslasuit-climate-control-system/

[20] M. Gabardi, D. Leonardis, M. Solazzi and A. Frisoli, "Development of a miniaturized thermal module designed for integration in a wearable haptic device," in *2018 IEEE Haptics Symposium (HAPTICS),* pp. 100-105, San Francisco, CA, 2018. doi: **https://doi.org/10.1109/HAPTICS.2018.8357160**

[21] T. Murakami, T. Person, C. L. Fernando and K. Minamizawa, "Altered touch: Miniature haptic display with force thermal and tactile feedback for augmented haptics", in *Proc. ACM SIGGRAPH Emerg. Technol. (Sigraph '17),* Article 53, 1-2, 2017. doi: **https://doi.org/10.1145/3102163.3102225**

[22] S. Günther, F. Müller, D. Schön, O. Elmoghazy, M. Mühlhäuser, and M. Schmitz, "Therminator: Understanding the Interdependency of Visual and On-Body Thermal Feedback in Virtual Reality," in *Proceedings of the 2020 CHI Conference on Human Factors in Computing Systems (CHI '20)*, Association for Computing Machinery, New York, NY, USA, 1–14, 2020. doi: **https://doi.org/10.1145/3313831.3376195**

[23] HaptX: Haptic gloves for VR training, simulation, and design. http://haptx.com/

[24] I. Choi, E. Ofek, H. Benko, M. Sinclair, and C. Holz, "Claw: A multifunctional handheld haptic controller for grasping, touching, and triggering in virtual reality," in *Proceedings of the 2018 CHI Conference on Human Factors in Computing Systems*, pp. 1-13. 2018. doi: **https://doi.org/10.1145/3173574.3174228**

[25] E. Whitmire, H. Benko, C. Holz, E. Ofek, and M. Sinclair, "Haptic revolver: Touch, shear, texture, and shape rendering on a reconfigurable virtual reality controller," in *Proceedings of the 2018 CHI Conference on Human Factors in Computing Systems*, pp. 1-12, 2018. doi: **https://doi.org/10.1145/3173574.3173660**

[26] H. Benko, C. Holz, M. Sinclair and E. Ofek, "Normaltouch and Texturetouch: High-fidelity 3d haptic shape rendering on handheld virtual reality controllers," in *Proceedings of the 29th Annual Symposium on User Interface Software and Technology*, pp. 717-728. 2016. doi: **https://doi.org/10.1145/2984511.2984526**

[27] B. C. M. Murray *et al*., "A variable shape and variable stiffness controller for haptic virtual interactions," in *2018 IEEE International Conference on Soft Robotics (RoboSoft)*, pp. 264-269, Livorno, 2018. doi: **https://doi.org/10.1109/ROBOSOFT.2018.8404930**

[28] A. Zenner and A. Krüger, "Shifty: A weight-shifting dynamic passive haptic proxy to enhance object perception in virtual reality," in *IEEE transactions on visualization and computer graphics*, vol. 23, no. 4, pp.1285-1294, April 2017. doi: **https://doi.org/10.1109/TVCG.2017.2656978**

[29] W. Provancher, "Creating greater VR immersion by emulating force feedback with ungrounded tactile feedback." *IQT Quarterly*, vol. 6, no. 2, pp.18-21, 2014.

[30] X. Guo, Y. Zhang, D. Wang and J. Jiao, "Absolute and discrimination thresholds of a flexible texture display," in *2017 IEEE World Haptics Conference (WHC)*, pp. 269-274, Munich, 2017. doi: **https://doi.org/10.1109/WHC.2017.7989913**

[31] J. C. Stevens and K. C. Choo, "Temperature sensitivity of the body surface over the life span," in *Somatosensory & Motor Research*, vol. 15 no.1, pp. 13-28, 1998. doi: **https://doi.org/10.1080/08990229870925**

[32] M. A. Srinivasnan and R. H. LaMotte, "Tactual discrimination of softness," in *Journal of Neurophysiology*, vol. 73, no. 1, pp 88-101, 1995. doi: **https://doi.org/10.1152/jn.1995.73.1.88**

[33] K. Fujita and H. Ohmori, "A new softness display interface by dynamic fingertip contact area control," in *5th World Multiconference on Systemics, Cybernetics and Informatics*, pp. 78-82, 2001.

[34] X. Dai, J. Colgate, and M. Peshkin, "LateralPaD: A surface-haptic device that produces lateral forces on a bare finger," in *2012 IEEE Haptics Symposium (HAPTICS),* pp. 7-14. Vancouver, BC, 2012. doi: **https://doi.org/10.1109/HAPTIC.2012.6183753**

[35] H. -N. Ho, "Material recognition based on thermal cues: Mechanisms and applications," in *Temperature,* vol. 5, no. 1, pp. 36-55, 2018. doi: **https://doi.org/10.1080/23328940.2017.1372042**

[36] Ino, S. Shimizu, T. Odagawa, M. Sato, M. Takahashi, T. Izumi, *et al*., "A tactile display for presenting quality of materials by changing the temperature of skin surface," in *Proceedings of 2nd IEEE International Workshop on Robot and Human Communication*, pp. 220-224, Tokyo, Japan, 1993. doi: **https://doi.org/10.1109/ROMAN.1993.367718**

[37] C. Pacchierotti, S. Sinclair, M. Solazzi, A. Frisoli, V. Hayward and D. Prattichizzo, "Wearable Haptic Systems for the Fingertip and the Hand: Taxonomy, Review, and Perspectives," in *IEEE Transactions on Haptics*, vol. 10, no. 4, pp. 580-600, Oct. – Dec., 2017. doi: **https://doi.org/10.1109/TOH.2017.2689006**

[38] K.O. Johnson, T. Yoshioka and F. Vega-Bermudez, "Tactile functions of mechanoreceptive afferents innervating the hand," in *Journal of Clinical Neurophysiology,* vol. 17, no. 6, pp. 539-558, 2000. doi: **https://doi.org/10.1097/00004691-200011000-00002**